Resonance Raman Spectroscopy of the Integral Quinol Oxidase Complex of *Sulfolobus acidocaldarius*†

Sandra Gerscher,‡ Susanne Döpner,‡ Peter Hildebrandt,*,‡ Michael Gleissner,§ and Günter Schäfer§

Max-Planck-Institut für Strahlenchemie, Postfach 101365, D-45413 Mülheim an der Ruhr, Federal Republic of Germany, and Institut für Biochemie, Medizinische Universität, Ratzeburger Allee 160, D-23538 Lübeck, Federal Republic of Germany

Received April 15, 1996; Revised Manuscript Received July 16, 1996⊗

ABSTRACT: The integral quinol oxidase complex of *Sulfolobus acidocaldarius* (DSM 639) was investigated by resonance Raman spectroscopy. The complex includes four heme *a* groups which constitute two functional entities, a_{587} and aa_3, containing two low-spin hemes and a low-spin as well as a high-spin heme, respectively. RR spectra were obtained from the fully oxidized and fully reduced states of the complex using different excitation wavelengths in the Soret band region in order to disentangle the contributions from the four heme groups. For the oxidized state, this approach allowed for the identification of two spectrally different types of heme *a* which were assigned to the bishistidine ligated hemes *a* of aa_3 and a_{587} (type II) and to the additional heme *a* of a_{587} which is ligated by a histidine and methionine (type I). The spectra of both heme *a* types differ substantially from that of beef heart cytochrome *c* oxidase. In particular, the formyl stretching modes of types II and I are upshifted by 8 and 15 cm^{-1}, respectively, implying a largely hydrophobic environment of the formyl groups in the quinol oxidase of *Sulfolobus*. Furthermore, the RR spectra of the oxidized state reveal the characteristic marker bands of a five-coordinated and a six-coordinated high-spin state, indicating that heme a_3 exists in a coordination equilibrium, which is in sharp contrast to the purely six-coordinated high-spin configuration of heme a_3 in any (quinol or cytochrome) oxidases studied so far. Also the formyl stretching mode of heme a_3 appears to be unusual as its frequency is substantially lower than in beef heart oxidase. In the fully reduced state, no heterogeneity of heme a_3 is observed and also the spectra of the various hemes *a* are nearly indistinguishable. Moreover, the formyl stretching vibrations of all hemes *a* and a_3 apparently coincide to one prominent peak at 1658 cm^{-1} characteristic for a non-hydrogen-bonded carbonyl group. This finding is unique compared to other aa_3 oxidases in which the formyl stretchings give rise to widely separated bands at ∼1610 and ∼1665 cm^{-1} for heme *a* and a_3, respectively. In both the oxidized and the reduced states, the spectra of the aa_3 entity in the integral complex differ significantly from those of the isolated aa_3 entity studied previously [Heibel, G., Anzenbacher, P., Hildebrandt, P., & Schäfer, G. (1993a) *Biochemistry 32*, 10878−10884], indicating substantial interactions between the various subunits of the integral complex.

The archaebacterium *Sulfolobus acidocaldarius* (DSM 639) grows aerobically at low pH and high temperature (Brock et al., 1972). This extremophilic organism is positioned on the deepest branch of the evolutionary tree, and thus, it might provide a mirror image of "archaic" bioenergetic machineries. Hence, a deeper knowledge of the structure and function of its enzymes in relation to those of eubacteria and eucaryotes is of particular interest for a better understanding of both evolutionary changes of specific enzyme systems as well as of their molecular functioning.

Our interest is focused on the respiratory chain of *S. acidocaldarius* which has been found to include a terminal quinol oxidase complex (Anemüller et al., 1985; Schäfer et al., 1990; Lübben et al., 1992; Schäfer et al., 1994; Lübben, 1995). Originally an aa_3-type oxidase from *Sulfolobus* was isolated as a single entity (Sox-aa_3) including two hemes (*a*, a_3) and one copper ion (Anemüller & Schäfer, 1989; Anemüller et al., 1992).[1] This entity was functionally intact since it oxidized the physiological reductant caldariella quinol. Later it was shown that the operon encoding the quinol oxidase includes more than one gene (Lübben et al., 1992). One of the additional gene products, subunit C, contains two further heme *a* groups, cytochrome a_{587}. Thus, the integral quinol oxidase, SoxABCD, which is built up by four subunits, includes not only a "cytochrome *c* oxidase"-like module (SoxA; SoxB; aa_3) but also a two-heme *a* containing entity (SoxC; a_{587}) which might be related to the mitochondrial cytochrome *c* reductase complex (Lübben et al., 1992, Schäfer et al., 1994). In this sense, SoxABCD would constitute a simplified version of complexes III and IV of eucaryotes. Figure 1 shows the putative topology of this complex and the arrangement of the various redox sites, suggesting a direct electron transfer from SoxC to SoxB. In fact, recent kinetic studies seem to indicate that there is an

† This work was supported by DFG Grants Scha-125/17-2 and 17-3 (to G.S.) and Hi-464/2-1 and 3-1 (P.H.). P.H. gratefully acknowledges the Heisenberg fellowship by the DFG.

* Correspondence should be addressed to this author.
‡ Max-Planck-Institut für Strahlenchemie.
§ Medizinische Universität.

⊗ Abstract published in *Advance ACS Abstracts,* September 1, 1996.

[1] Abbreviations: BOX, beef heart cytochrome *c* oxidase; EPR, electron paramagnetic resonance; POX, cytochrome *c* oxidase of *Paracoccus denitrificans*; RR, resonance Raman; S/N, signal to noise; SOX, terminal quinol oxidase of *Sulfolobus acidocaldarius*; SoxABCD, integral oxidase complex of *Sulfolobus* including the a_{587} and aa_3 entities; Sox-aa_3, minimal form of SOX containing only the aa_3 entity; 6cLS, six-coordinated low spin; 6cHS, six-coordinated high spin; 5cHS, five-coordinated high spin.

S0006-2960(96)00896-3 CCC: $12.00

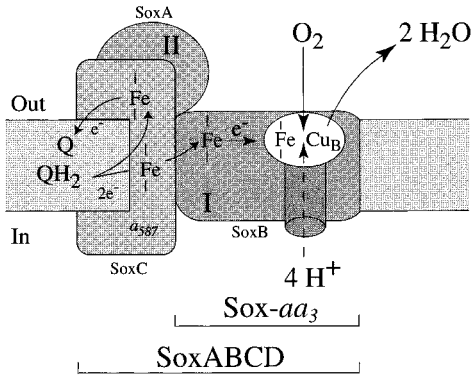

FIGURE 1: Schematic representation of the putative topology of the terminal oxidase complex of *S. acidocaldarius*, including the subunits SoxA, SoxB, and SoxC. The small subunit SoxD has been omitted.

efficient interaction between the a_{587} and the aa_3 sites, at least, as far as the electron flow is concerned (Giuffré et al., 1994). Monitoring the characteristic absorption bands at 603 and 587 nm, it was found that in the intact membrane both the aa_3 and the a_{587} entities are reduced quasisimultaneously by exogeneous reductants (ascorbate plus *N*,*N*,*N*′,*N*′-tetramethyl-*p*-phenylenediamine or dithionite) and rapidly reoxidized by oxygen.

In order to gain more insight into the structure of this enzyme complex, spectroscopic techniques have to be employed (Anemüller & Schäfer, 1989; Anemüller et al., 1992; Hildebrandt et al., 1991; Heibel et al., 1993a; Gerscher et al., 1995). Among them, resonance Raman (RR) spectroscopy is a particularly powerful tool since it selectively probes the vibrational pattern of the heme groups, thereby providing information about the molecular structure of the redox sites (Babcock, 1988). In continuation of our previous investigations of the "single entity" oxidase Sox-aa_3 (Hildebrandt et al., 1991; Heibel et al., 1993a) we have now investigated the integral four hemes *a*-containing complex SoxABCD in order to analyze the structural and functional communication between both entities in SoxABCD.

MATERIALS AND METHODS

Protein Purification and Sample Preparation. *S. acidocaldarius* (DSM 639) was grown in a mineral salt medium (Brock et al., 1972) as described by Anemüller and Schäfer (1990). Cells were suspended in 50 mM 2-(*N*-morpholino)-ethanesulfonate, pH 5.5 at 4 °C and centrifuged for 15 min at 7800*g*, and the pellets were resuspended in the same buffer. Membranes of *S. acidocaldarius* were prepared by disrupting the cells as described in Anemüller and Schäfer (1990). Membranes were washed with a buffer containing 30 mM $Na_4P_2O_7$ and solubilized by dodecyl maltoside with a 1.2:1 (w/w) detergent:protein ratio. The SoxABCD complex was purified to homogeneity by a method combining hydrophobic interaction and anion-exchange chromatography. On a denaturing polyacrylamide gel (15% SDS) this complex shows four bands. Details of this procedure will be published elsewhere (Gleissner & Schäfer, unpublished results). For the RR experiments, the protein sample was diluted by a buffer (pH 7.3) containing 25 mM Tris-HCl, 150 mM NaCl, and 0.3 mM dodecyl maltoside to yield an optical density of 1.5 at the excitation wavelength. The fully reduced complex was prepared by addition of a small amount of dithionite. While an essentially complete conversion to the reduced state was possible, protein samples from some batches could not be completely converted to the fully oxidized state using various oxidizing agents [potassium ferricyanide, cerium(IV) sulfate]. In these preparations, a fraction of the sample remained in the reduced state as indicated by the intensity distribution for characteristic oxidation state marker bands ν_4 at ~1360 and ~1370 cm^{-1} for the reduced and oxidized hemes, respectively. The contribution of the reduced state to the measured RR spectrum, which was up to 30% in terms of relative RR band intensities of the ν_4 modes, was removed by an appropriate subtraction of the RR spectrum of the fully reduced complex using these marker bands as well as the formyl stretching bands as references. The resultant spectra revealed no differences as compared to those obtained from completely oxidizable samples, indicating that the reduced hemes refer to all hemes of a fraction of the enzyme rather than to specific hemes of all enzyme molecules. Thus, such spectra were combined with those of the completely oxidizable samples to improve the overall signal-to-noise (S/N) ratio for the RR spectrum of the fully oxidized state.

RR Measurements. RR spectra were measured with the output of a Kr^+ laser (413 or 407 nm) or a He/Cd laser (442 nm) using a double monochromator equipped with a photon counting system. The spectral resolution was 2.8 cm^{-1} and the step width (increment per data point) was 0.2 cm^{-1}. The S/N ratio was improved upon repetitive scanning so that the total accumulation time was between 30 and 70 s per data point. The resetability of the monochromator during the experiments was ± 0.1 cm^{-1} as repeatedly checked by calibration against the position of the laser line. The sample was deposited in a rotating cell to avoid photoreduction and photoinduced damage. All measurements were carried out at ambient temperature. Further details of the experimental setup are described elsewhere (Heibel et al., 1993b; Hildebrandt et al., 1993). The RR spectra of Sox-aa_3 and beef heart cytochrome *c* oxidase (BOX) shown in this work were obtained as described previously (Heibel et al., 1993a,b).

The single scan spectra of each experiment were carefully compared and only combined if no spectral differences were noted. The spectra obtained in this way included a continuous and structureless background which was removed by polynomial subtraction. The spectra were analyzed by a band-fitting program as described elsewhere (Hildebrandt et al., 1993).

RESULTS AND DISCUSSION

The RR spectroscopic measurements were restricted to the region between 1300 and 1700 cm^{-1}. This spectral range includes the so-called marker bands of the porphyrin whose frequencies are characteristic for the oxidation, spin, and ligation state of the heme and the internal stretching vibrations of the vinyl and formyl substituents which are sensitive toward interactions with the protein environment (Kitagawa & Orii, 1977; Babcock & Salmeen, 1979; Choi et al., 1983; Ching et al., 1985; Parthasarathi et al., 1987; Kitagawa & Ozaki, 1987; Babcock, 1988; Sassaroli et al., 1989; Heibel et al., 1993b). Thus, this region appears to be most appropriate to study multiheme enzymes such as oxidases.

RR spectroscopy of SOX complexes is aggravated by a relatively intense scattering background (Hildebrandt et al.,

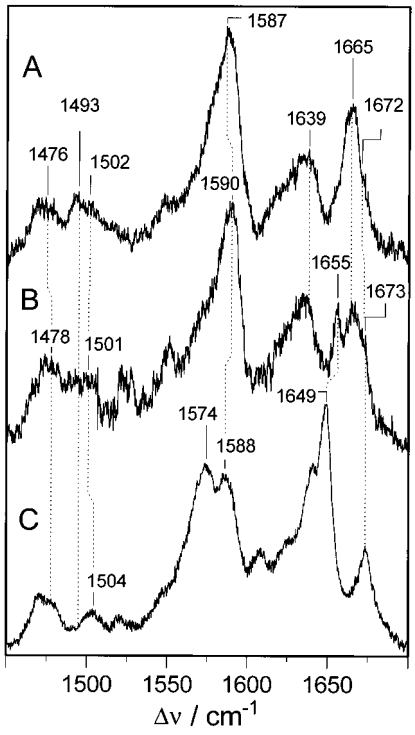

FIGURE 2: RR spectra of SoxABCD (A), Sox-aa_3 (B), and BOX (C) in the fully oxidized state excited at 413 nm.

1991; Heibel et al., 1993a). Thus a long accumulation time of up to 24 h was required to obtain spectra of the quality shown in this work. Furthermore, the background slowly increased during the RR experiments, presumably due to the formation of larger aggregates so that the samples had to be replaced by fresh ones after about 2 h. Due to these severe experimental constraints, our investigations were focused onto the fully oxidized and the fully reduced complexes by using various excitation wavelengths.

RR Spectra of the Fully Oxidized State. Figure 2A shows the RR spectra of the fully oxidized SoxABCD complex. There are striking differences compared to the RR spectrum of BOX (Figure 2C) such as the lack of the strong band at 1649 cm^{-1} and the much weaker intensity of the 1672-cm^{-1} band, which both are located in the region of the formyl stretching modes. Furthermore, the ν_2 band region (1570−1590 cm^{-1}) shows only a weak shoulder at ∼1574 cm^{-1} whereas BOX reveals a pronounced peak at this position. In this respect, the spectrum of SoxABCD is more closely related to that of the Sox-aa_3 single entity form (Figure 2B).

In the region of the ν_3 mode both SOX complexes exhibit a band at ∼1493 cm^{-1} which is particularly pronounced in the RR spectrum of SoxABCD and has no counterpart in the RR spectrum of BOX. The assignment of this band to a residual amount of reduced oxidase which would give rise to a band close to this position can be ruled out since the ν_4 band region between 1340 and 1380 cm^{-1} (not displayed in the figure) reveals only a single band at 1370 cm^{-1} (ferric heme) but no shoulder at the low frequency side, which would be characteristic for ferrous heme. Thus, the 1493-cm^{-1} band is attributed to the ν_3 mode of a ferric heme, which in model compounds appears at 1482, 1492, and 1506 cm^{-1} in six-coordinated high-spin (6cHS), five-coordinated high-spin (5cHS), and six-coordinated low-spin (6cLS) species, respectively (Parthasarathi et al., 1987). Therefore, the 1493-cm^{-1} band must be due to a 5cHS state while the nearby peaks at 1476 and 1502 cm^{-1} correspond to 6cHS and 6cLS hemes, respectively. This assignment is in line with the RR spectrum of the cyanide-bound SoxABCD complex (not shown). Binding of cyanide leads to a conversion of the HS forms to a 6cLS configuration and, hence, should be reflected by the disappearance of both the 1493 and the 1476 cm^{-1} bands, which is in fact observed. Since the 5cHS configuration is found in the RR spectra of both SoxABCD and Sox-aa_3, it must originate from the aa_3 entity. Thus, these findings imply that heme a_3 exists in a coordination equilibrium between a 5cHS and 6cHS state. The present results confirm the conclusion drawn from our previous study on the single entity Sox-aa_3 (Heibel et al., 1993a).

The RR spectra of SoxABCD include contributions from five different species, which are two 6cLS hemes *a* of the a_{587} entity and the 6cLS heme *a*, as well as the 5cHS and 6cHS states of heme a_3 of the aa_3 entity. Therefore, about 50 different bands may contribute to the measured RR spectra in this region. In an attempt to simplify the analysis of the SoxABCD spectra, we tried to subtract the contribution of the aa_3 entity (i.e., Figure 2: spectrum A minus spectrum B). However, the characteristic 1493-cm^{-1} band (5cHS of heme a_3) could not be removed without producing artifacts (negative peaks) in the difference spectra. Thus, individual contributions to the RR spectra of the hemes *a* and a_3 or/and the coordination equilibrium of heme a_3 within the aa_3 entity in the intact SoxABCD complex are different from those in the isolated Sox-aa_3.

Variation of the Excitation Wavelength. We attempted to disentangle the RR spectra of SoxABCD, choosing different excitation wavelengths which may preferentially enhance the RR bands of the individual hemes (Ching et al., 1985; Heibel et al., 1993b). Unfortunately, excitation lines in the Q-band region, which might provide the highest selectivity, could not be employed due to a strong background scattering which completely obscured the RR signals. Therefore, our experiments were restricted to excitation in the Soret band region. Sections of such spectra are shown in Figure 3.

The inspection of these data reveals that variation of the excitation wavelength leads to a redistribution of the RR intensities, thereby causing shifts of the apparent peak maxima. For instance, in the ν_2 band and C═O stretching regions the main peaks are at 1590 and 1657 cm^{-1} in the 442- and 407-nm excited spectra, but at 1587 and 1664 cm^{-1} in the spectrum excited at 413 nm. These spectral changes can be used to resolve the overlapping peaks into terms of the dominant components. Employing a band-fitting analysis in the first step, we tried to simulate each spectrum with a minimum number of bands. In the second step, these results were compared to obtain a set of bands which are sufficient for a fit of all the spectra using constant frequencies and half-widths but variable band intensities. Finally, this set of bands was iteratively refined to yield the best global fit for all spectra. In this way, the degrees of freedom in the fitting procedure were significantly reduced [cf. Döpner et al. (1996)] so that the peaks could be resolved into individual components. As the number of bands required for the global fit is less than the total number of modes expected to contribute to the spectra, some of the resolved components may not represent pure vibrational bands of an individual

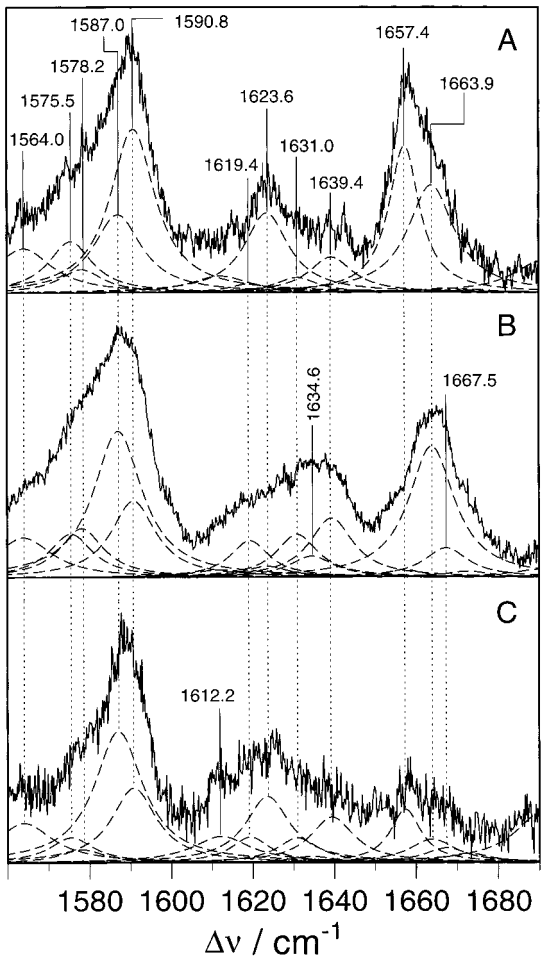

FIGURE 3: RR spectra of the fully oxidized complex SoxABCD excited at 407 nm (A), 413 nm (B), and 442 nm (C). The dashed lines represent the fitted Lorentzian band shapes.

heme, rather then an overlap of two or more unresolvable bands.

For the broad and asymmetric peaks at ~1580 cm^{-1} in the three spectra, four bands between 1575 and 1590 cm^{-1} are required for a satisfactory fit. These bands are in the region of the ν_2 mode, and according to their frequencies, two of them (1587.0, 1590.8 cm^{-1}) are characteristic for a 6cLS configuration and two of them (1575.5, 1578.2 cm^{-1}) for HS species (Babcock, 1988; Heibel et al., 1993b). Hence, the latter bands are readily attributed to the 6cHS and 5cHS conformers of heme a_3. In the region between 1634 and 1640 cm^{-1} two bands at 1634.6 and 1639.4 cm^{-1} are required to simulate the spectra. Based on their frequencies these bands are readily assigned to the ν_{10} modes of 6cLS hemes. In a previous study of BOX it was found that for the 6cLS heme *a* the intensity ratio of this mode with respect to the ν_2 mode is largely the same at 407- and 413-nm excitation (Heibel et al., 1993b). Using this criterion, the 1634.6- and 1639.4-cm^{-1} bands are related to the ν_2 modes at 1587.0 and 1590.8 cm^{-1}, respectively. Similarly, there are at least three bands in the C═O stretching region between 1650 and 1680 cm^{-1}. The band at 1667.5 cm^{-1} is at a frequency close to that attributed to the HS species in Sox-aa_3. Such an assignment is also supported by a comparison of the relative band intensities (with respect to ν_2 mode) which are similar in BOX at both 413- and 407-nm excitation (Heibel et al., 1993b). Hence, the alternative assignment of the 1657- and 1664-cm^{-1} bands to the formyl stretching of the HS species would imply that this mode is up to 20 times more intense than the ν_2 modes. Consequently, the bands at 1657.4 and 1663.9 cm^{-1} can be assigned to those 6cLS hemes which give rise to the bands at 1590.8 and 1587.0 cm^{-1}, respectively. Further assignments which are based on similar arguments are given in Table 1. As indicated above, several other bands may include contributions from different modes of the various hemes such as the bands at 1619.4 cm^{-1} [ν_{10} (5cHS), $\nu_{C=C}$ (5cHS, 6cHS)] and 1564.0 cm^{-1} [ν_{38x} (6cLS, 6cHS, 5cHS)] and, hence, do not represent individual modes but must be regarded as overlaps of several closely spaced bands.

In spite of the uncertainties of the fitting procedure and the band assignment, it is evident that the spectrum of SoxABCD includes contributions of two spectrally different types of 6cLS hemes *a* (I, II), in addition to those of the 6cHS and 5cHS species of heme a_3. SoxABCD, however, contains three 6cLS hemes, which means that two of them are indistinguishable in the present RR spectra. It is tempting to identify these two hemes as those of the a_{587} moiety since they are located in the same protein subunit (Schäfer et al., 1994). Moreover, these hemes constitute a functional unit which appears reminiscent to mitochondrial cytochrome *b* of the bc_1 complex, which contains two structurally similar hemes *b*. Still, magnetic circular dichroism experiments have provided strong evidence that the two hemes in cytochrome a_{587} show different ligation patterns (Spinner et al., 1994). While one heme a_{587} is coordinated by two histidines like the heme *a* of the aa_3 entity, the second heme a_{587} is bound by a histidine and a methionine ligand. Thus, an alternative and more likely assignment to the type I and II hemes *a* is based on the ligation pattern, i.e., His-His vs His-Met ligation.

Further support for this assignment comes from the absorption spectra (Figure 4). In the oxidized spectra (Figure 4A) there is a substantial red shift of the composite peaks from 421 nm in Sox-aa_3 to 426 nm in SoxABCD in the Soret band region and from 597 nm in Sox-aa_3 to 601 nm in SoxABCD in the Q-band region. The spectrum (Figure 4B) of the reduced state, however, shows a slight blue shift of the composite peaks from 439 nm in Sox-aa_3 to 436 nm in SoxABCD in the Soret band region. In the Q-band region the band of Sox-aa_3, which is centered at 601 nm, is replaced by two bands at 587 and 603 nm in SoxABCD. As all heme groups of the *Sulfolobus* SoxABCD have the same chemical structure (Lübben et al., 1994), it is reasonable to assume that the main contribution to the new features in the absorption spectrum of SoxABCD originates from the uniquely ligated heme *a* of the a_{587} entity. Since the RR intensities are governed by both the ground state and the excited state properties, the intensity variations of the conjugate modes of the type I and II hemes *a* (e.g., ν_2; see Figure 3) are likely to reflect the differences of the Soret transitions between His-Met- and His-His-ligated hemes *a*. Thus, for the oxidized state excitation at the low-wavelength side of the Soret peak, i.e., at 407 nm, should lead to a preferential enhancement of the modes of the His-His-ligated hemes *a* of aa_3 and a_{587} while those of the His-Met-ligated heme *a* are expected to become stronger at 442-nm excitation. This enhancement pattern should hold in particular for the A_{1g} modes. In fact, the intensities of 1587.0- and 1590.8-cm^{-1} bands (ν_2) vary in the expected manner with the latter being the stronger one at 407-nm excitation but the weaker

Table 1: Assignments for Fully Oxidized *Sulfolobus* and Beef Heart Oxidases[a]

	SoxABCD				Sox-aa_3			BOX	
	I(a)[b]	II(a)[b]	a_3		a	a_3		a	a_3
mode	6cLS	6cLS	6cHS	5cHS	6cLS	6cHS	5cHS	6cLS	6cHS
ν_{28}	1469.0	1464.6			1472.1			1470.1	
ν_3	1501.5		1476.4	1492.6	1499.9	1480.9	1491.1	1499.1	1479.6
ν_{38y}					1528.1	1505.0		1528.4	1505.0
ν_{11}	1547.2		1518.8		1542.8	1521.3		1545.9	1520.1
ν_{38x}	1564.0				1564.1	1550.9		1566.9	1557.8
ν_2	1587.0	1590.8	1575.5	1578.2	1588.6	1575.4	1583.3	1589.9	1574.8
ν_{37}						1592.3		1603.7	1584.7
ν_{10}	1634.6	1639.4	1612.2		1636.0	1608.9		1639.2	1609.2
$\nu_{C=C}$	1631.0	1623.6	1619.4		1627.3	1619.8		1626.8	1619.7
$\nu_{C=O}$	1663.9	1657.4	1667.5		1655.4	1665.8		1649.0	1673.6

[a] The vibrational assignments for Sox-aa_3 and BOX refer to Heibel et al. (1993a,b). The assignments for SoxABCD are discussed in the text. Frequencies are given in cm^{-1}. [b] Tye I and II hemes *a* refer to the His-Met and His-His-ligated hemes, respectively.

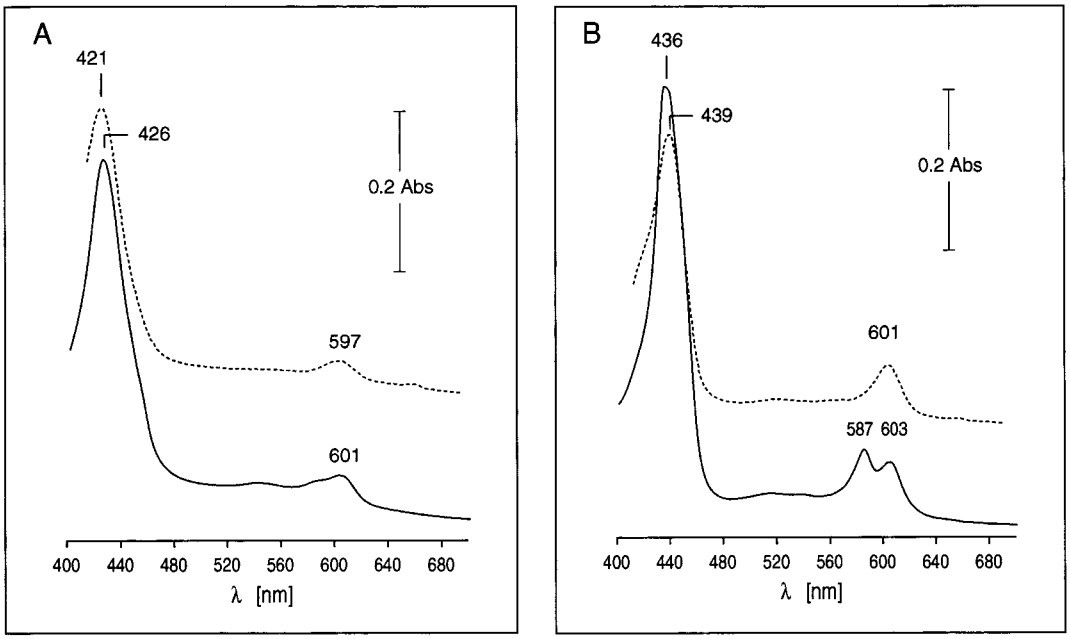

FIGURE 4: Oxidized (A) and fully reduced (B) absorption spectra of SoxABCD (—) and Sox-aa_3 (- - -) from *S. acidocaldarius*. Concentrations of 1.3 μM were determined for SoxABCD (1 μM for Sox-aa_3) by using a differential absorption coefficient of 24.4 (20.8) mM^{-1} cm^{-1} at "604 nm minus 630 nm".

one at longer excitation wavelengths. Thus, the 1587.0-cm^{-1} band (type I) is attributed to the His-Met-ligated heme *a* of the a_{587} entity while the 1590.8-cm^{-1} band (type II) must originate from the His-His-ligated hemes *a* of both the aa_3 and the a_{587} entities.

The most pronounced spectral differences between both types of heme *a* refer to the porphyrin mode ν_{10} and the formyl stretching. The 6.5-cm^{-1} frequency difference of the latter reflects different interactions with the protein environment. In the type I heme *a*, the carbonyl group is presumably less strongly hydrogen bonded than in type II heme *a*, which shows a similar frequency as heme *a* of the isolated Sox-aa_3 entity. The mode ν_{10} is known to be a sensitive marker for deviations from the planar heme geometry (Alden et al., 1989; Czernuszewicz et al., 1989). For a largely planar structure of 6cLS heme, this mode is expected at ~1640 cm^{-1} as it is observed for the type II heme *a* as well as for BOX (Heibel et al., 1993b). Ruffling-type distortions cause a downshift of this mode so that the frequency decrease of this mode by 5 cm^{-1} in type I heme *a* may indicate a nonplanar porphyrin geometry as it has been observed for *Paracoccus denitrificans* cytochrome *c* oxidase (POX). Alternatively, the shift of the ν_{10} modes may just reflect the different ligation pattern in type I heme *a* (Teraoka & Kitagawa, 1980).

RR Spectra of the Fully Reduced Complex. The RR spectrum of the fully reduced SoxABCD complex (Figure 5A) differs even more from that of Sox-aa_3 (Figure 5B) and BOX (Figure 5C) as compared to the fully oxidized species. These differences are particularly pronounced in the formyl stretching region above 1600 cm^{-1}. In BOX, these modes are largely separated for the heme a_3 (1665 cm^{-1}) and the heme *a* group (1610 cm^{-1}) while in Sox-aa_3 the latter is upshifted to 1657 cm^{-1}. The corresponding heme a_3 mode remains at a similar frequency; however, its intensity is drastically reduced. The 1610-cm^{-1} band is also missing in SoxABCD, but in contrast to Sox-aa_3 there is only a single band at 1658 cm^{-1} which has become the strongest RR band of all at 413-nm (and 407-nm) excitation.[2] Its intensity is about twice as high as that of the ν_2 envelope at 1589 cm^{-1}, which indicates that the formyl stretching modes of all four

[2] RR spectra of the fully reduced SoxABCD obtained with 407- and 442-nm excitation are not shown in this work.

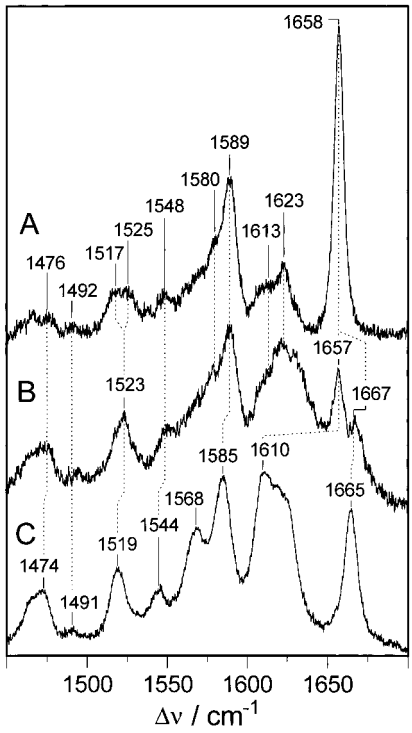

FIGURE 5: RR spectra of SoxABCD (A), Sox-aa_3 (B), and BOX (C) in the fully reduced state excited at 413 nm.

heme groups accidentally coincide. It is noteworthy that the 1658-cm^{-1} peak is readily fitted by a single Lorentzian line shape (fit not shown).

Apparently, also most of the porphyrin modes of the various hemes *a* are congruent. Attempts to resolve the RR spectra by use of various excitation lines were not as successful as in the case of the fully oxidized enzyme. Although changes of the relative intensities of the peaks were noted, the underlying bands of the hemes *a* apparently vary in a similar manner so that a spectral discrimination is not possible. The only exception refers to the ν_{11} mode which corresponds to single bands at 1523 and 1519 cm^{-1} in Sox-aa_3 and BOX, respectively. In SoxABCD this mode is replaced by a broad peak exhibiting two components at 1517 and 1525 cm^{-1}. As the intensity ratio of both bands (I_{1525}/I_{1517}) is much larger at 407- than at 413- or 442-nm excitation,[2] the 1525-cm^{-1} band is tentatively assigned to the type I heme *a* (His-Met-ligated heme) since in the fully reduced state the Soret band envelope of SoxABCD is blue shifted compared to Sox-aa_3 (Figure 4B). This mode is known to respond to alterations of the electron density in the porphyrin which may be affected by the axial ligands (Partharasathi et al., 1987). Thus, a frequency shift of this mode in the His-Met-ligated heme *a* compared to His-His-ligated hemes *a* is not surprising. The band-fitting analysis, however, provides no evidence for further structural heterogeneity between the heme *a* groups.

Compared to the joint heme *a* bands, those of the heme a_3 group are relatively weak at all excitation wavelengths used in this study. The only band which is unambiguously attributed to heme a_3 is the mode ν_3 at 1476 cm^{-1} which is at the same position as in Sox-aa_3 and close to that of BOX. Furthermore, the shoulder at ca. 1580 cm^{-1} may, at least partially, be due to the ν_2 mode of this heme. Thus, we have no indication for an unusual structure or coordination pattern of the reduced heme a_3, which, hence, may exist in a 5cHS configuration as in BOX.

Redox-Linked Structural Changes. Studies of iron porphyrin *a* model compounds have shown that reduction generally leads to a downshift of the formyl stretching by ~25 cm^{-1} for a 6cLS heme, in both a protic or an aprotic environment (Babcock & Callahan, 1983; Babcock, 1988; Han et al., 1991). For HS hemes a_3, these shifts are smaller (~10 cm^{-1}). Thus, one may conclude that substantially larger or smaller shifts reflect redox-linked changes of the hydrogen-bonding interactions and/or changes of the heme structure which in turn may affect the coupling between the formyl stretching and the porphyrin vibrations. For example, a strengthening of the hyrogen bonds upon reduction has been invoked to explain the large downshift of this heme *a* formyl stretching in BOX from 1649 to 1610 cm^{-1} while the carbonyl group of the heme a_3 remains in a hydrophobic environment (Babcock & Callahan, 1983). The heme *a* groups of SOX reveal an unusual behavior because they exhibit a much smaller (Met-His heme *a*) or even no downshift (His-His heme *a*). This indicates that hydrogen-bonding interactions are weaker and/or vibrational coupling between the formyl groups and the porphyrin skeletons is diminished in all heme *a* groups. Evidently, the reduction of the heme groups causes similar structural changes of all heme *a* sites. The formyl stretching of heme a_3, however, reveals a downshift which is normal compared to BOX or HS heme a_3 model compounds. Alternatively, one might argue that the coincidence of this mode with those of the heme *a* groups is due to the conversion of heme a_3 from a 5cHS to a 6cLS configuration, caused by binding of an exogeneous ligand. In fact, in the cyanide-bound reduced heme a_3 of the ba_3 oxidase of *Thermus thermophilis*, the C═O stretching is at the same position, i.e., at 1657 cm^{-1} (Oertling et al., 1994). However, this interpretation can be ruled out as the marker band ν_3 is found at 1476 cm^{-1}, which is at a position characteristic for a HS configuration of a ferrous heme a_3. Moreover, there are no indications for an unusual behavior of the porphyrin modes of heme a_3 in the fully reduced state at all.

Effect of Protein−Protein Interactions in SoxABCD. One cannot subtract the contribution of the aa_3 entity from the spectra of SoxABCD (Figures 2A and 5A), using the measured RR spectra of Sox-aa_3 (cf. Figures 2B and 5B), which suggests that the environment of the aa_3 sites is modified in SoxABCD due to protein−protein interactions. In the fully oxidized state, the main effect of these interactions is readily identified as a shift of the coordination equilibrium of heme a_3. Taking the intensity ratio of the ν_3 modes of both heme a_3 states (~1476 and 1493 cm^{-1}; Figure 2) as a measure for the concentration ratio, it can easily be seen that the 5cHS fraction has clearly increased in Sox-ABCD as compared to Sox-aa_3. It is not possible to decide whether or not also the heme *a* site reveals structural differences between both oxidase preparations because the bands originating from both His-His-ligated hemes *a* within the aa_3 and the a_{587} entities cannot be distinguished. However, electron paramagnetic resonance (EPR) data suggest that also the heme *a* within the aa_3 entity is affected. While the EPR spectrum of oxidized Sox-aa_3 is very similar to that of BOX and shows one LS signal at $g_{zyx} = 3.02, 2.21, 1.45$ (Anemüller & Schäfer, 1992), for SoxABCD three LS heme *a* signals are observed which are lower than those of Sox-aa_3 (Lübben et al., 1994). Also in the fully reduced

state, unambiguous differences between SoxABCD and Sox-aa_3 refer to the heme a_3 as its formyl stretching frequency (1667 cm^{-1}) is downshifted in the integral complex but remains unchanged in Sox-aa_3. Thus, one would expect that the underlying protein−protein interactions may particularly affect the processes associated with the heme a_3 site, e.g., oxygen binding.

Structure−Function Relationships. It is tempting to relate the structural differences of the heme sites of the aa_3 moiety in Sox-aa_3 and SoxABCD as compared to mitochondrial and bacterial cytochrome *c* oxidases to different reaction mechanisms or functions (Musser et al., 1993). The fact that a different reductant (quinol instead of cytochrome *c*) is used is *per se* not likely to account for these differences since the RR spectrum of the quinol oxidizing aa_3 complex of *Bacillus subtilis* agrees very well with that of BOX (Lauraeus & Wikström, 1992). Structural differences between quinol and cytochrome *c* type oxidases which are related to the intermolecular electron transfer process may be restricted to reductant binding sites and the Cu_A center which is missing in quinol oxidases (Musser et al., 1993). However, both sites are not probed by RR spectroscopy. Hence, the unique structural properties of the heme *a* and heme a_3 groups which become evident by the present study may be put down as adaptations to the extreme living conditions of *S. acidocaldarius* which impose specific requirements for electron transfer, oxygen binding, and putative proton pumping, as well as the membrane environment.

The recently determined crystal structures of the oxidized cytochrome *c* oxidases BOX and POX do not identify a sixth axial ligand for heme a_3 (Tsukihara et al., 1995; Iwata et al., 1995). Moreover, the Fe ion is displaced from the heme plane by 0.7 Å toward the fifth histidine ligand (Iwata et al., 1995) as it is characteristic for a 5cHS configuration (Koenig, 1965; Hoard et al., 1965). In contrast, the RR spectra of BOX or POX in solution clearly indicate an in-plane geometry of the heme a_3 iron corresponding to a 6cHS configuration (Babcock, 1988; Heibel et al., 1993b). Although this discrepancy must be taken with caution as the resolution of the crystal structure is 2.8 Å (Iwata et al., 1995), it may well be that subtle perturbations imposed by the crystal packing lead to structural changes at the heme a_3 site, implying that the ligation state of this heme is sensitively controlled by details of the protein conformation. There is hardly any sequence homology between this subunit I of BOX (and POX) and the Sox-aa_3 polypeptide, but the amino acid residues forming the metal binding sites in both proteins are highly conserved (Lübben et al., 1992). Thus, it is neither surprising nor an indication for a preparation artifact as suspected previously (Heibel et al., 1993a) that in SoxABCD and Sox-aa_3 the 5cHS configuration is already significantly populated in solution. In fact, in order to enable oxygen binding, the sixth ligand has to be released from heme a_3. Moreover, in view of the apparent sensitivity of the coordination equilibrium from protein conformation it is easy to understand that the most pronounced effect of protein−protein interactions between the a_{587} and the aa_3 entities is observed in a shift of the heme a_3 coordination equilibrium.

It is more difficult to rationalize the redox-linked structural changes which include all heme groups or at least their formyl substituents. With respect to the hemes of the aa_3 moiety it is again instructive to refer to the crystal structure of BOX (and POX) which indicates that there is one transmembrane helix (TM 10), which provides contacts with both heme *a* and heme a_3 (Tsukihara et al., 1995; Iwata et al., 1995). Moreover, this helix includes Phe-377 (BOX) which is part of the peptide segment His-Phe-His providing axial ligands for both heme groups. If this part of the polypeptide structure is similar in Sox-aa_3, one may imagine that a dislocation of this helix can induce structural changes in both heme centers. Alternatively, it may be envisaged that it is just the reduction of heme a_3 which causes a displacement of the tripeptide segment. This movement might lead to a slight reorientation of heme *a* putting its formyl substituent in a more hydrophobic environment.

The a_{587} entity of SoxABCD exhibits two midpoint potentials closely spaced around $+240 \pm 20$ mV (Schäfer et al., 1994). Thus, it may well be that in the integral complex this two-heme center constitutes the primary acceptor for electrons from caldariella quinol since the midpoint potential of the latter in solution is less positive (+106 mV). A possible scheme for the reaction of caldariella quinol and the SoxABCD complex is shown in Figure 1. The most striking structural property of the a_{587} entity is the Met-His ligation of one of the hemes. In this respect, it is related to *bd* quinol oxidase of *Escherichia coli*. In this enzyme, heme *b* which serves as the electron acceptor for ubiquinol has been shown to be ligated by a His and a Met residue (Spinner et al., 1995). This structural similarity suggests that it is the His-Met-ligated heme *a* of SoxABCD which serves as the entry for the electrons. It remains to be shown whether both hemes of the a_{587} subunit constitute a Q-loop mechanism and which of the hemes serves as an electron donor for the aa_3 site.

In any case, due to the lack of a Cu_A site heme *a* is the primary electron acceptor of the aa_3 subunit. However, under physiological conditions it may receive electrons from the a_{587} site rather than directly from the quinol (Figure 1). This would constitute a fundamental functional difference from other quinol oxidases studied so far. Consequently, the unique structural properties of this heme *a* and the redox-linked conformational changes of its formyl substituent may reflect the specific requirements of an intramembrane electron pathway. Then the direct reduction of the isolated Sox-aa_3 by caldariella quinol (Anemüller & Schäfer, 1990) may either represent a facultative or a nonphysiological electron transfer process.

ACKNOWLEDGMENT

We thank Professor K. Schaffner for encouragement and support.

REFERENCES

Alden, R. G., Crawford, B. A., Doolen, R., Ondrias, M. R., & Shelnutt, J. A. (1989) *J. Am. Chem. Soc. 111*, 2070−2072.

Anemüller, S., & Schäfer, G. (1989) *FEBS Lett. 244*, 451−455.

Anemüller, S., & Schäfer, G. (1990) *Eur. J. Biochem. 191*, 297−305.

Anemüller, S., Lübben, M., & Schäfer, G. (1985) *FEBS Lett. 193*, 83−87.

Anemüller, S., Bill, E., Schäfer, G., Trautwein, X., & Teixeira, M. (1992) *Eur. J. Biochem. 210*, 133−138.

Babcock, G. T. (1988) in *Biological Applications of Raman Spectroscopy* (Spiro, T. G., Ed.) pp 293−346, Wiley, New York.

Babcock, G. T., & Callahan, P. M. (1983) *Biochemistry 22*, 2314−2319.

Brock, T. D., Brock, K. M., Belly, R. T., & Weiss, R. L. (1972) *Arch. Mikrobiol. 84*, 54−68.
Ching, Y.-C., Argade, P. V., & Rousseau, D. L. (1985) *Biochemistry 24*, 4938−4946.
Choi, S., Lee, J. J., Wei, Y. H., & Spiro, T. G. (1983) *J. Am. Chem. Soc. 105*, 3692−3707.
Czernuszewics, R. S., Li, X.-Y., & Spiro, T. G. (1989) *J. Am. Chem. Soc. 111*, 7024−7031.
Döpner, S., Hildebrandt, P., Mauk, A. G., Lenk, H., & Stempfle, W. (1996) *Spectrochim. Acta A 51*, 573−584.
Gerscher, S., Döpner, S., Hildebrandt, P., Gleissner, M., & Schäfer, G. (1995) *J. Inorg. Biochem. 59*, 283.
Giuffré, A., Antonini, G., Brunori, M., D'Itri, E., Malatesta, F., Nicoletti, F., Anemüller, S., Gleissner, M., & Schäfer, G. (1994) *J. Biol. Chem. 269*, 31006−31011.
Han, S., Ching, Y.-C., Hammes, S. L., & Rousseau, D. L. (1991) *Biophys. J. 60*, 45−52.
Heibel, G., Anzenbacher, P., Hildebrandt, P., & Schäfer, G. (1993a) *Biochemistry 32*, 10878−10884.
Heibel, G., Hildebrandt, P., Ludwig, B., Steinrücke, P., Soulimane, T., & Buse, G. (1993b) *Biochemistry 32*, 10866−10877.
Hildebrandt, P., Heibel, G., Anemüller, S., & Schäfer, G. (1991) *FEBS Lett. 283*, 131−134.
Hildebrandt, P., Vanhecke, F., Buse, G., Soulimane, T., & Mauk, A. G. (1993) *Biochemistry 32*, 10912−10922.
Hoard, J. L., Hamor, M. J., Hamor, T. A., & Caughey, W. S. (1965) *J. Am. Chem. Soc. 87*, 2312−2319.
Iwata, S., Ostermeier, C., Ludwig, B., & Michel, H. (1995) *Nature 376*, 660−669.
Kitagawa, T., & Orii, Y. (1978) *J. Biochem. (Tokyo) 84*, 1245−1252.
Kitagawa, T., & Ozaki, Y. (1987) *Struct. Bonding 64*, 71−114.
Koenig, D. F. (1965) *Acta Crystallogr. 18*, 663−673.
Lauraeus, M., & Wikström, M. (1992) *Biochemistry 31*, 10054−10060.
Lübben, M. (1995) *Biochim. Biophys. Acta 1229*, 1−22.
Lübben, M., Kolmerer, B., & Saraste, M. (1992) *EMBO J. 11*, 805−812.
Lübben, M., Warne, A., Albracht, S. P. J., & Saraste, M. (1994) *Mol. Microbiol. 13*, 327−335.
Musser, S. M., Stowell, M. H. B., & Chan, S. I. (1993) *FEBS Lett. 327*, 131−136.
Oertling, W. A., Surerus, K. K., Einarsdóttir, Ó., Fee, J. A., Dyer, R. B., & Woodruff, W. H. (1994) *Biochemistry 33*, 3128−3141.
Parthasarathi, N., Hansen, C., Yamaguchi, S., & Spiro, T. G. (1987) *J. Am. Chem. Soc. 109*, 3865−3871.
Sassaroli, M., Ching, Y.-C., Dasgupta, S., & Rousseau, D. L. (1989) *Biochemistry 28*, 3128−3132.
Schäfer, G., Lübben, M., & Anemüller, S. (1990) *Biochim. Biophys. Acta 1018*, 271−274.
Schäfer, G., Anemüller, S., Moll, R., Gleissner, M., & Schmidt, C. (1994) *Syst. Appl. Microbiol. 16*, 544−555.
Spinner, F., Cheeseman, M. R., Watmous, N. J., Greenwood, C., Thomson, A. J., Gleissner, M., Anemüller, S., & Schäfer, G. (1994) *EBEC Short Rep. 8*, 45.
Spinner, F., Cheesman, M. R., Thomson, A. J., Kaysser, T., Gennis, R. B., Peng, Q., & Peterson, J. (1995) *Biochem. J. 308*, 641−644.
Teraoka, J., & Kitagawa, T. (1980) *J. Phys. Chem. 84*, 1928−1935.
Tsukihara, T., Aoyama, H., Yamashita, E., Tomizaki, T., Yamaguchi, H., Shinzawa-Itoh, K., Nakashima, R., Yaono, R., & Yoshikawa, S. (1995) *Science 269*, 1069−1074.

BI960896D